Cervical Spinal Cord Degeneration in Spinocerebellar Ataxia Type 7

C.R. Hernandez-Castillo, R. Diaz, T.J.R. Rezende, I. Adanyeguh, I.H. Harding, F. Mochel, and J. Fernandez-Ruiz

ABSTRACT

BACKGROUND AND PURPOSE: Spinocerebellar ataxia type 7 is an autosomal dominant neurodegenerative disease caused by a cytosine-adenine-guanine (CAG) repeat expansion. Clinically, spinocerebellar ataxia type 7 is characterized by progressive cerebellar ataxia, pyramidal signs, and macular degeneration. In vivo MR imaging studies have shown extensive gray matter degeneration in the cerebellum and, to a lesser extent, in a range of cortical cerebral areas. The purpose of this study was to evaluate the impact of the disease in the spinal cord and its relationship with the patient's impairment.

MATERIALS AND METHODS: Using a semiautomated procedure applied to MR imaging data, we analyzed spinal cord area and eccentricity in a cohort of 48 patients with spinocerebellar ataxia type 7 and compared them with matched healthy controls. The motor impairment in the patient group was evaluated using the Scale for Assessment and Rating of Ataxia.

RESULTS: Our analysis showed a significantly smaller cord area ($t = 9.04$, $P < .001$, $d = 1.31$) and greater eccentricity ($t = -2.25$, $P = .02$, $d = 0.32$) in the patient group. Similarly, smaller cord area was significantly correlated with a greater Scale for Assessment and Rating of Ataxia score ($r = -0.44$, $P = .001$). A multiple regression model showed that the spinal cord area was strongly associated with longer CAG repetition expansions ($P = .002$) and greater disease duration ($P = .020$).

CONCLUSIONS: Our findings indicate that cervical spinal cord changes are progressive and clinically relevant features of spinocerebellar ataxia type 7, and future investigation of these measures as candidate biomarkers is warranted.

ABBREVIATIONS: CAG = cytosine-adenine-guanine; SARA = Scale for Assessment and Rating of Ataxia; SCA7 = spinocerebellar ataxia type 7

Spinocerebellar ataxia type 7 (SCA7) is a neurodegenerative disease characterized by cerebellar ataxia, pyramidal signs, and retinal dystrophy.[1] SCA7 is caused by the expansion of a cytosine-adenine-guanine (CAG) repeat that lies in the coding region of in the *ATXN7* gene on chromosome 3p12-13.[2] Patients with SCA7 may eventually develop other neurologic deficits, including loss of manual dexterity, dysarthria, dysphagia, and eye-movement abnormalities.[1]

Olivopontocerebellar atrophy associated with SCA7 has been documented in different neuropathologic studies using both postmortem and in vivo imaging techniques. These techniques have identified severe gray matter degeneration in a broad range of cerebellar and cerebral regions, including the cerebellar cortex, the inferior olivary complex tracts, the subthalamic nucleus, the pallidum, and the substantia nigra.[3] Similarly, MR imaging studies in SCA7 reported extensive cerebellar degeneration and, to a lesser extent, in cortical cerebral regions such as the pre-/postcentral gyri, cuneus, precuneus, inferior occipital gyrus, insula, and inferior frontal gyrus.[4-6] However, studies of the central nervous system to date in SCA7 have focused primarily on brain changes, overlooking the possible involvement of spinal cord degeneration on the motor deficits caused by the disease. A number of reports in other ataxias have shown a strong association between spinal cord and the motor deficits that the patients develop, including Friedreich ataxia,[7] SCA1,[8] and SCA3.[9]

Received February 5, 2021; accepted after revision April 12.

From the Faculty of Computer Science (C.R.H.-C.), Dalhousie University, Halifax, Nova Scotia, Canada; Physiology Department, Faculty of Medicine (R.D., J.F.-R.), Universidad Nacional Autónoma de México, Cuidad de Mexico, Mexico; Department of Neurology and Neuroimaging Laboratory (T.J.R.R.), School of Medical Sciences, University of Campinas, São Paulo, Brazil; Institut national de la santé et de la recherche médicale, Centre national de la recherche scientifique, Sorbonne Universités, Paris Brain Institute, Paris, France; Department of Neuroscience (I.H.), Central Clinical School, Monash University, Melbourne, Australia; and Department of Genetics (F.M.), Assistance Publique–Hôpitaux de Paris, Pitié-Salpêtrière University Hospital, Paris, France.

This work was supported by Consejo Nacional de Ciencia y Tecnología grant No. A1-S-10669 and Programa de Apoyo a Proyectos de Investigación e Innovación Tecnológica - Universidad Nacional Autónoma de México grant No. IN220019 to Juan Fernandez-Ruiz.

Please address correspondence to Juan Fernandez-Ruiz, MD, PhD, Departmento de Fisiologia, Facultad de Medicina, Universidad Nacional Autónoma de México, Av. Universidad 3000, A.P. 70-250, C.P. 04510, CDMX, Mexico; e-mail: jfr@unam.mx

Indicates article with online supplemental data.

http://dx.doi.org/10.3174/ajnr.A7202

Table 1: Demographics and descriptive statistics

	SCA7 ($n = 48$)	Healthy Controls ($n = 48$)	*P* Value
Age (mean) (yr)	40.02 (SD, 14.1)	42.31 (SD, 13.61)	.452
Sex (M/F)	26:22	26:22	1.000
Disease duration (mean) (yr)	9.52 (SD, 6.3)	NA	NA
Spinal cord area (mean) (mm^2)	49.45 (SD, 7.7)	63.39 (SD, 7.2)	<.001
Spinal cord eccentricity (mean)	0.75 (SD, 0.07)	0.72 (SD, 0.05)	.026
CAG (mean)	46.72 (SD, 6.1)	NA	NA
SARA (mean)	14.79 (SD, 8.6)	NA	NA

Note:—NA indicates not applicable.

Here, using structural MR images that cover the brain and upper spinal cord, collected using standard clinical protocols, we systematically measured in vivo spinal cord degeneration in a large cohort of patients with SCA7 and matched healthy controls from Mexico and France. We aimed to investigate the hypothesis that SCA7 is associated with decreased cervical spinal cord area and increased spinal cord eccentricity (flattening) and that these measures are associated with ataxia severity. Our results will show the potential use of spinal cord morphology as an MR imaging biomarker for SCA7 progression.

MATERIALS AND METHODS

Subjects

The data set used in this study was previously reported in separate studies for both the Universidad Nacional Autonoma de Mexico and the Pitié-Salpêtrière University Hospital.[6,10,11] The final sample (48 patients) included 38 patients from Mexico and 10 patients from France. For each site, age- and sex-matched healthy volunteers were invited to participate as a control group. General demographics can be found in Table 1. All participants gave their informed consent before entering the study, and all the procedures in this study were conducted in accordance with the international standards dictated by the Helsinki Declaration of 1964. Additionally, all the procedures were performed in accordance with the ethical standards of the committees on human experimentation of the Universidad Nacional Autonoma de Mexico and by the Comité de Protection des Personnes-Ile de France Paris VI, respectively.

Clinical Assessment

We used the Scale for the Assessment and Rating of Ataxia (SARA) to measure the motor impairment in the patient group. The clinical evaluation was performed either the day of the scanning or within a week from the scanning session. The SARA score comprises 8 items, including tests of gait, stance, sitting, and speech, as well as the finger-chase test, finger-to-nose test, rapid alternating movements, and heel-to-shin test.[12] The score ranges from 0 to 40, with a higher score indicating a greater impairment.

Image Acquisition

Images from the Mexican subset were acquired using a 3T Achieva MR imaging scanner (Phillips Healthcare) and a 32-channel head coil. The anatomic sequence consisted of a 3D T1 fast-field echo sequence, with a TR/TE = 8/3.7 ms, FOV = 256 × 256 mm, and reconstruction matrix = 256 × 256, resulting in an isometric resolution of 1 mm. The images from the French subset were acquired using a 3T Magnetom Trio scanner (Siemens) and a standard transmit body coil (Siemens) and a 32-channel receive head coil array. The anatomic sequence consisted of a 3D MPRAGE volumetric image with TR = 2530 ms, TE = 3.65 ms, TI = 900 ms, flip angle = 9°, and FOV = 256 × 256 mm, resulting in an isometric resolution of 1 mm.

Spinal Cord Measurement

All the image analyses were implemented in Matlab R2020b (MathWorks). To minimize any systematic differences between scanners, we created a model using an independent set of MR imaging data of healthy subjects from both the Mexican ($n = 20$) and French ($n = 20$) sites. In this model, we assigned a different regressor per site. Then, we regressed out the respective site coefficients from the data used in this study before any processing. The spinal cord segmentation was then performed using the Spinal Cord Toolbox, Version 5.0.1 (SCT; www.spinalcordtoolbox.com)[13] and the ENIGMA-Ataxia pipeline (http://enigma.ini.usc.edu/ongoing/enigma-ataxia/) for spinal cord analysis. In brief, the SCT provides a preprocessing platform to segment and normalize automatically the spinal cord into a template, correcting for variations in imaging angle and neck position. Then morphologic metrics of the normalized cross-sections of the spinal cord were obtained for statistical analysis.

On the basis of previous reports,[8,9] we selected the base (lower limit) of the second and third cervical vertebrae, defined by the location of the relevant intraverterbral discs, for further analysis. The selection of the cervical vertebrae in the normalized images required manual intervention. This step was performed by an expert using a graphic interface in which the base of the vertebra of interest was identified in the sagittal plane of the T1 image for each subject. We estimated the mean values of the cross-sectional area and eccentricity of the spinal cord from the analysis of 3 consecutive slices for each vertebra following a validated procedure.[14] These 2 metrics provide different morphologic information—eg, the cross-sectional area can be used to evaluate the overall degeneration, while the eccentricity provides an approximation of the flattening of the cord section.

Statistical Analysis

Statistical tests were performed in Matlab R2020b. Normal distribution of the metrics was evaluated using the Kolmogorov-Smirnov test. We used a Student *t* test to identify significant group differences in the spinal cord area and eccentricity of each vertebra, and we report effect size using the Cohen D. Then to test the association between the SARA score and the morphologic metrics in the SCA7 group, we used the Pearson correlation. To control for the variable rate of decline in disease progression as

predicted by the CAG repeat length, we used a multiple regression model to evaluate the effects of CAG repetition expansion and disease duration on the morphology of the spinal cord. Finally, to further explore the association of the spinal cord area and the disease progression, we calculated the Pearson correlation between disease burden and the spinal cord area. The disease burden was calculated as the interaction between the CAG expansion and age. Then we split the patient group into early (<5 years from onset), middle (>5 and <10 years from onset), and late (>10 years from onset) stages, based on the distribution of our sample and to try to get similar group sizes for visualization.

RESULTS

Descriptive statistics of the patients and healthy volunteers can be found in Table 1. The spinal cord area in patients with SCA7 was significantly smaller than in the healthy volunteers (Fig 1) in both C2 ($t = 9.04$, $P = <.001$, $d = 1.31$) and C3 ($t = 8.96$, $P = <.001$, $d = 1.25$). The spinal cord eccentricity was only significantly different in C2 ($t = -2.25$, $P = .02$, $d = 0.32$). Spinal cord segmentation of an exemplary subject of each group can be found in the Online Supplemental Data. We found a strong association between the cord area and the SARA score (Fig 2) in both C2 ($r = -0.44$, $P = .001$) and C3 ($r = -0.39$, $P = .005$). We found no association between the cord eccentricity and the SARA score ($P = .896$). Finally, our multiple variable regression showed that the cord area was associated with CAG repetition expansion (coefficient = −1.09, $P = .002$) and disease duration (coefficient = −3.72, $P = .02$), while the cord eccentricity was not significantly associated with either of the 2 independent variables (Table 2). We found a strong negative correlation between disease burden and spinal cord area ($r = -0.41$, $P = .003$), suggesting that the spinal cord area is reduced during disease progression. This was more evident when we grouped the patients on the basis of the disease duration. Figure 3 shows that patients in the early stage have a significantly smaller area than the control group ($t = 2.88$, $P = .005$, $d = 0.66$) but a larger area than those in the middle and late stages ($t = 2.39$, $P = .02$, $d = 0.86$).

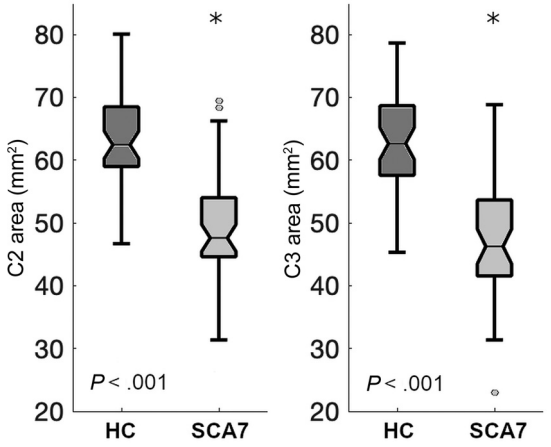

FIG 1. Spinal cord cross-sectional area in patients with SCA7 and healthy controls (HC). The *asterisks* indicate significant difference.

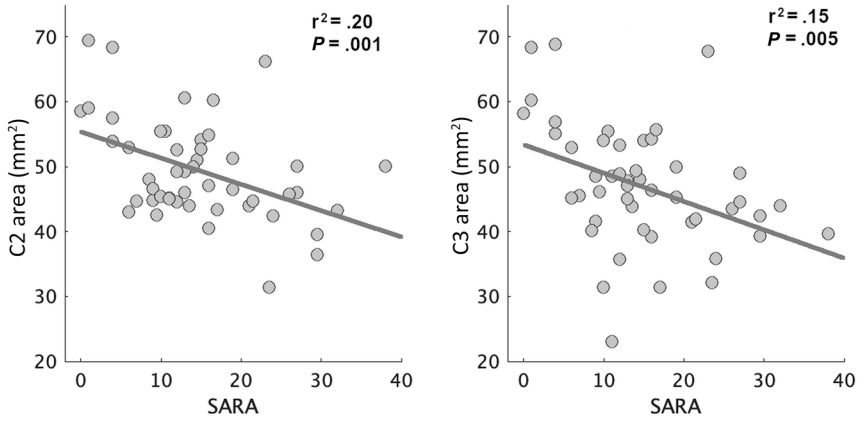

FIG 2. Association between the spinal cord cross-sectional area and the SARA score. Each *dot* represents 1 patient with SCA7

DISCUSSION

In this study, we report that cervical spinal cord degeneration is a robust feature of the manifestation of SCA7 and is significantly associated with disease severity and duration. These findings support the potential for readily quantifiable MR imaging measures of the spinal cord area to provide biomarkers that allow tracking of the degenerative process in SCA7. The methods used herein enable accurate measurement of the spinal cord using clinically standard brain MR imaging acquisitions. Our results provide the first in vivo corroboration of postmortem neuropathologic reports of spinal atrophy in SCA7[15] and additionally reveal associations between spinal morphology and disease severity. Bang et al,[4] in 2004, suggested that the degenerative process in SCA7 starts in the brainstem, even before the patients develop ataxia. Only when the cerebellar degeneration becomes prominent do patients develop motor impairment. Given the association between spinal cord atrophy and cerebellar dysfunction in our patient group, it is possible that spinal cord degeneration occurs parallel to cerebellar degeneration, affecting the communication between the cerebellum and motor neurons in the peripheral nervous system. Further investigation using other image modalities, such as diffusion MR imaging, and longitudinal data sets could provide evidence regarding the degenerative mechanism in SCA7 and other ataxias.

Our analysis also revealed differences with previous reports in other SCAs. For example, a strong association between the cord area and the CAG expansion was found in SCA1[8] and SCA7, but not in SCA3.[9] Similarly, different amounts of spinal cord flattening (assessed by the cord eccentricity) have been reported in those 3 subtypes.[7-9] Flattening of the spinal cord generally reflects the targeted atrophy of ≥1 spinal tract (eg, ascending dorsal sensory tracts versus descending ventral motor tracts). The finding of robust reductions in total spinal cord area, along with more modest changes in eccentricity,

Table 2: Results of the multiple variable regression

Dependent Variable	r^2 Model	Independent Variable	Regression Coefficient	*P* Value
Spinal cord area	0.27	CAG	–1.09	.002
		Disease duration	–3.72	.020
		CAG*DD	2.24	.029
Spinal cord eccentricity	0.07	CAG	1.64	.107
		Disease duration	1.24	.218
		CAG*DD	–1.36	.178

Note:—CAG*DD indicates CAG multiplied by disease duration.

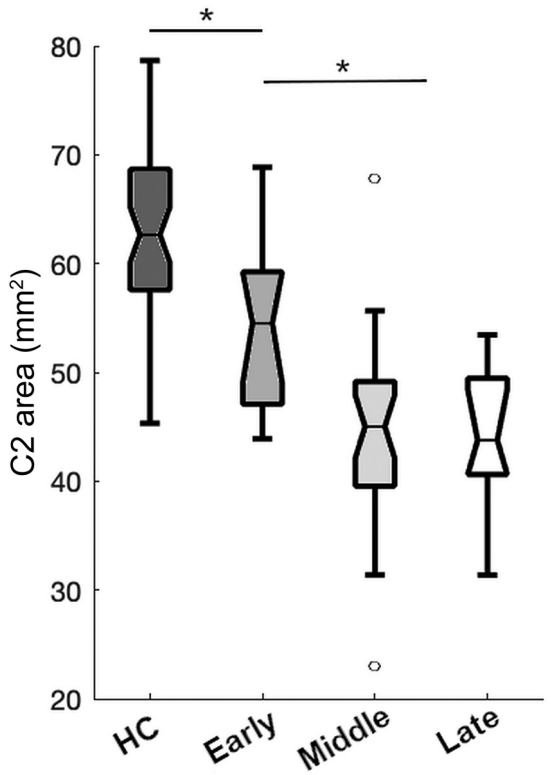

FIG 3. Spinal cord cross-sectional area for healthy controls (HC) and patients with SCA7 subdivided by disease burden (see Materials and Methods). The *asterisks* indicate significant difference.

may reflect a more generalized pattern of spinal atrophy. Such differences between different SCAs should be further explored on a larger scale to identify whether different areas of the spinal cord are susceptible to specific mutations, an effect that has been reported in the cerebellar cortex.[10]

A limitation of this study is that our current analysis is limited to a specific cross-sectional area (see Materials and Methods). For example, in our cohort, we found flattening in the cervical region around the second vertebra but no significant difference around the third vertebra, suggesting different degrees of morphologic changes across levels in the spinal cord. New analytic techniques that analyze the spinal cord in a voxelwise fashion could provide a more detailed mapping of spinal cord degeneration caused by SCA7. Similarly, the use of other MR imaging modalities such as diffusion-weighted imaging can provide relevant information regarding the integrity of the fibers, a metric that could be more sensitive to the degenerative process. Although our data indicate a clear progressive degeneration, we cannot assess or rule out the potential contribution of developmental hypoplasia to the overall between-group differences. Furthermore, we correlated spine atrophy with the SARA score, which is widely used to assess disease severity in patients with spinocerebellar ataxia. However, the SARA score was not specifically designed to assess pyramidal dysfunction; hence, future studies of spinal degeneration can benefit from using clinical measures of pyramidal tract alterations and sensory deficits.

CONCLUSIONS

SCA7 is characterized by extensive spinal cord degeneration that is associated with the disease severity. The cervical cross-sectional area in the patients is highly related to CAG repetition expansion and disease duration. Hence, spinal cord morphometry provides a compelling candidate for use as a potential MR imaging biomarker of SCA7 progression.

Disclosures: Ian Harding—*UNRELATED*: *Employment*: Monash University, *Comments*: my employer as an academic scientist. Fanny Mochel—*RELATED*: *Grant*: Programme hospitalier de recherche clinique BIOSCA-ID RCB: 2010-A01324-35, AOM10094, NCT01470729.* Jaun Fernancex-Ruiz—*RELATED*: *Grant*: Consejo Nacional de Ciencia y Tecnología grant No. A1-S-10669 and Programa de Apoyo a Proyectos de Investigación e Innovación Tecnológica - Universidad Nacional Autónoma de México grant No. IN220019.* *Money paid to the institution.

REFERENCES

1. Hugosson T, Gränse L, Ponjavic V, et al. **Macular dysfunction and morphology in spinocerebellar ataxia type 7 (SCA 7).** *Ophthalmic Genet* 2009;30:1–6 CrossRef Medline
2. Garden GA, La Spada AR. **Molecular pathogenesis and cellular pathology of spinocerebellar ataxia type 7 neurodegeneration.** *Cerebellum* 2008;7:138–49 CrossRef Medline
3. Martin JJ. Spinocerebellar ataxia type 7. In: Subramony SL, Dürr A, eds. *Handbook of Clinical Neurology*. Vol 103. Elsevier; 2012:475–91
4. Bang OY, Lee PH, Kim SY, et al. **Pontine atrophy precedes cerebellar degeneration in spinocerebellar ataxia 7: MRI-based volumetric analysis.** *J Neurol Neurosurg Psychiatry* 2004;75:1452–56 CrossRef Medline
5. Döhlinger S, Hauser TK, Borkert J, et al. **Magnetic resonance imaging in spinocerebellar ataxias.** *Cerebellum* 2008;7:204–14 CrossRef Medline
6. Hernandez-Castillo CR, Galvez V, Diaz R, et al. **Specific cerebellar and cortical degeneration correlates with ataxia severity in spinocerebellar ataxia type 7.** *Brain Imaging Behav* 2016;10:252–57 CrossRef Medline
7. Chevis CF, Da Silva CB, D'Abreu A, et al. **Spinal cord atrophy correlates with disability in Friedreich's ataxia.** *Cerebellum* 2013;12:43–47 CrossRef Medline
8. Martins CR, Martinez AR, de Rezende TJ, et al. **Spinal cord damage in spinocerebellar ataxia type 1.** *Cerebellum* 2017;16:792–96 CrossRef Medline
9. Fahl CN, Branco LM, Bergo FP, et al. **Spinal cord damage in Machado-Joseph disease.** *Cerebellum* 2015;14:128–32 CrossRef Medline
10. Hernandez-Castillo CR, King M, Diedrichsen J, et al. **Unique degeneration signatures in the cerebellar cortex for spinocerebellar ataxias 2, 3, and 7.** *Neuroimage Clin* 2018;20:931–38 CrossRef Medline

11. Adanyeguh IM, Perlbarg V, Henry P-G, et al. **Autosomal dominant cerebellar ataxias: imaging biomarkers with high effect sizes.** *Neuroimage Clin* 2018;19:858–67 CrossRef Medline
12. Schmitz-Hübsch T, Du Montcel ST, Baliko L, et al. **Scale for the assessment and rating of ataxia: development of a new clinical scale.** *Neurology* 2006;66:1717–20 CrossRef Medline
13. De Leener B, Lévy S, Dupont SM, et al. **SCT: Spinal Cord Toolbox, an open-source software for processing spinal cord MRI data.** *Neuroimage* 2017;145:24–43 CrossRef Medline
14. Bergo FPG, França MC, Chevis CF, et al. **SpineSeg: a segmentation and measurement tool for evaluation of spinal cord atrophy.** In: *7th Iberian Conference on Information Systems and Technologies (CISTI 2012)*, Madrid, Spain, June 20-23, 2012:1–4
15. Martin JJ, Krols L, Ceuterick C, et al. **On an autosomal dominant form of retinal-cerebellar degeneration: an autopsy study of five patients in one family.** *Acta Neuropathol* 1994;88:277–86 CrossRef Medline